Performance of shortcut-to-adiabaticity quantum engines

Obinna Abah[1] and Eric Lutz[2,3]

[1]*Centre for Theoretical Atomic, Molecular and Optical Physics, Queen's University Belfast, Belfast BT7 1NN, United Kingdom*

[2]*Department of Physics, Friedrich-Alexander-Universität Erlangen-Nürnberg, D-91058 Erlangen, Germany*

[3]*Institute for Theoretical Physics I, University of Stuttgart, D-70550 Stuttgart, Germany*

(Received 1 August 2017; revised manuscript received 28 August 2018; published 17 September 2018)

We consider a paradigmatic quantum harmonic Otto engine operating in finite time. We investigate its performance when shortcut-to-adiabaticity techniques are used to speed up its cycle. We compute efficiency and power by taking the energetic cost of the shortcut driving explicitly into account. We analyze in detail three different shortcut methods: counterdiabatic driving, local counterdiabatic driving, and inverse engineering. We demonstrate that all three lead to a simultaneous increase of efficiency and power for fast cycles, thus outperforming traditional heat engines.

DOI: 10.1103/PhysRevE.98.032121

I. INTRODUCTION

Heat engines have been a cornerstone of thermodynamics since the seminal work of Carnot almost 200 years ago. Carnot established that the efficiency of an engine, defined as the ratio of energy output to energy input, is maximal for quasistatic processes [1,2]. Maximum efficiency is, however, associated with vanishing power, the rate of work production, since the quasistatic limit requires that the engine cycle is completed in an infinitely long time. For practical purposes, heat engines operate in finite time at finite power [3,4]. There is generally a trade-off between power and efficiency in this context [5]: increasing power leads to a decrease of efficiency, and vice versa [6–9]. A current challenge is to design energy efficient thermal machines that deliver more output for the same input, without sacrificing power [10].

Promising techniques to achieve this goal are collectively known as shortcuts to adiabaticity (STA). STA protocols are nonadiabatic processes that reproduce in finite time the same final state as that of an infinitely slow adiabatic process [11,12]. These methods have been successfully demonstrated on a large number of experimental platforms. Examples include high-fidelity driving of a Bose-Einstein condensate (BEC) [13], fast transport of trapped ions [14–16], fast adiabatic passage using a single spin in diamond [17] and cold atoms [18,19], as well as swift equilibration of a Brownian particle [20]. Different approaches to STA have been developed, such as counterdiabatic driving (CD), where a global term is added to the system Hamiltonian to compensate for nonadiabatic transitions [21–23], local counterdiabatic driving (LCD), where the counterdiabatic term is mapped onto a local potential [24,25], and inverse engineering (IE) based on the use of dynamical invariants [26,27] (see Ref. [11] for a review).

Shortcut-to-adiabaticity methods have lately been employed to enhance the performance of classical and quantum heat engines, by reducing irreversible losses that suppress efficiency and power [28–33]. However, the energetic cost of the STA driving [34–39] has not been taken into account in these studies. We have recently computed efficiency and power of a quantum harmonic Otto engine by properly including these costs, defined as the time average of the expectation value of the STA term, for the case of LCD [40]. We have found that LCD allows one to simultaneously increase efficiency and power for fast engine cycles, thus leading to energy efficient quantum thermal machines.

In this paper, we extend this previous investigation to two other STA methods, namely, CD and IE, and compare their respective capabilities. We specifically compute efficiency and power of a STA quantum Otto heat engine cycle whose working medium is a time-dependent harmonic oscillator, a paradigmatic model for a quantum thermal machine [7,8]. For each STA protocol, we explicitly evaluate the cost of the STA driving for compression and expansion phases of the engine cycle. We find that all three STA methods allow us to increase, at the same time, efficiency and power for fast cycles. We additionally show that the IE approach outperforms both CD and LCD, as it results in the largest efficiency and power enhancement.

II. QUANTUM OTTO ENGINE

We consider an Otto cycle for a time-dependent quantum harmonic oscillator. The corresponding Hamiltonian is of the standard form, $H_0(t) = p^2/(2m) + m\omega_t^2 x^2/2$, where x and p are the position and momentum operators of an oscillator of mass m. As shown in Fig. 1, the cycle is made of the following steps: (i) an isentropic compression branch (AB) where the oscillator is isolated and its frequency ω_t is unitarily increased from ω_1 to ω_2 in a time τ_1; (ii) a hot isochoric branch (BC) where heat is transferred from the hot bath at inverse temperature β_2 to the oscillator in a time τ_2 at fixed frequency; (iii) an isentropic expansion branch (CD) where the frequency is modulated to decrease from ω_2 to ω_1 in a time τ_3; and (iv) a cold isochoric branch (DA) where heat is transferred from the oscillator to the cold bath at inverse temperature $\beta_1 > \beta_2$ in a time τ_4. The frequency is again kept constant. The control parameters are the time allocations on

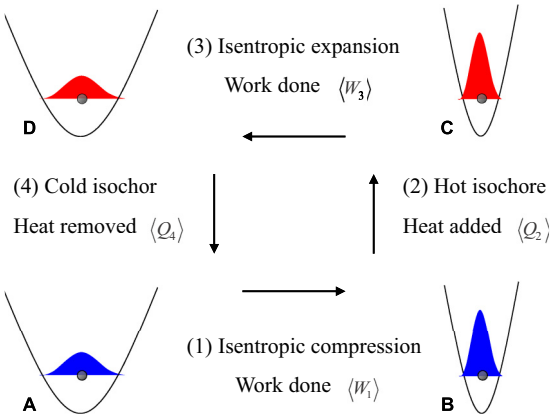

FIG. 1. Quantum Otto cycle of a harmonic oscillator with time-dependent frequency. The thermodynamic cycle consists of two unitary (compression and expansion steps 1 and 3) and two isochoric processes (heating and cooling steps 2 and 3).

the different branches, the temperatures of the baths, and the extreme values of the modulated frequency. We assume, as is commonly done [7,8,41–45], that the thermalization times $\tau_{2,4}$ are much shorter than the compression and expansion times $\tau_{1,3}$. The total cycle time is then $\tau_{\rm cycle} = \tau_1 + \tau_3 = 2\tau$ for equal step duration.

During the first and third strokes (compression and expansion), the quantum oscillator is isolated and only work is performed by changing the frequency in time. Since the dynamic is unitary, the Schrödinger equation for the parametric harmonic oscillator can be solved exactly for any given frequency modulation [46,47]. The corresponding work values are given by [8]

$$\langle W_1 \rangle = \frac{\hbar}{2}(\omega_2 Q_1^* - \omega_1) \coth\left(\frac{\beta_1 \hbar \omega_1}{2}\right), \tag{1}$$

$$\langle W_3 \rangle = \frac{\hbar}{2}(\omega_1 Q_3^* - \omega_2) \coth\left(\frac{\beta_2 \hbar \omega_2}{2}\right), \tag{2}$$

where we have introduced the dimensionless adiabaticity parameter Q_i^* $(i = 1, 3)$ [48]. It is defined as the ratio of the mean energy and the corresponding adiabatic mean energy and is thus equal to 1 for adiabatic processes [47]. Its explicit expression for any frequency modulation ω_t may be found in Refs. [46,47]. On the other hand, the heat exchanged with the reservoirs during the thermalization step (the hot isochoric process) reads

$$\langle Q_2 \rangle = \frac{\hbar \omega_2}{2}\left[\coth\left(\frac{\beta_2 \hbar \omega_2}{2}\right) - Q_1^* \coth\left(\frac{\beta_1 \hbar \omega_1}{2}\right)\right]. \tag{3}$$

For an engine, the produced work is negative, $\langle W_1 \rangle + \langle W_3 \rangle < 0$, and the absorbed heat is positive, $\langle Q_2 \rangle > 0$.

The dynamics of the quantum Otto engine may be sped up with the help of STA techniques applied to the compression and expansion steps. The STA protocols suppress the unwanted nonadiabatic transitions and thereby reduce the associated entropy production [6–9]. The effective Hamiltonian of the oscillator is then of the form

$$H_{\rm eff}(t) = H_0(t) + H^i_{\rm STA}(t), \tag{4}$$

where $H^i_{\rm STA}(t)$ is the STA driving Hamiltonian and $i = 1, 3$ indicates the respective compression or expansion step. The STA protocol satisfies boundary conditions which ensure that initial and final expectation values $\langle H^i_{\rm STA}(0, \tau)\rangle$ vanish:

$$\begin{aligned} &\omega(0) = \omega_i, \quad \dot\omega(0) = 0, \quad \ddot\omega(0) = 0, \\ &\omega(\tau) = \omega_f, \quad \dot\omega(\tau) = 0, \quad \ddot\omega(\tau) = 0, \end{aligned} \tag{5}$$

where $\omega_{i,f} = \omega_{1,2}$ denotes the respective initial and final frequencies of the compression and expansion steps. Conditions (5) are, for example, satisfied by [12,24,25]

$$\begin{aligned} \omega(t) = \omega_i + 10(\omega_f - \omega_i)s^3 - 15(\omega_f - \omega_i)s^4 \\ + 6(\omega_f - \omega_i)s^5, \end{aligned} \tag{6}$$

where we have introduced $s = t/\tau$.

Efficiency and power are the two main quantities characterizing the performance of a heat engine. The efficiency indicates how well the input energy (heat) is converted into the output energy (work), while the power specifies the rate at which the output energy is produced [2]. For a STA engine, the energy input is increased by the energy needed to implement the shortcut. As a result, we define the efficiency of a STA engine as [40]

$$\eta_{\rm STA} = \frac{\text{energy output}}{\text{energy input}} = \frac{-(\langle W_1 \rangle_{\rm STA} + \langle W_3 \rangle_{\rm STA})}{\langle Q_2 \rangle + \langle H^1_{\rm STA} \rangle_\tau + \langle H^3_{\rm STA} \rangle_\tau}, \tag{7}$$

where $\langle H^i_{\rm STA} \rangle_\tau = (1/\tau)\int_0^\tau dt \langle H^i_{\rm STA}(t)\rangle$ is the time average of the mean STA driving. Equation (7) takes the energetic cost of the STA driving along the compression and expansion steps into account. It reduces to the adiabatic efficiency $\eta_{\rm AD}$ in the absence of these two contributions (note that $\eta_{\rm STA} \leqslant \eta_{\rm AD}$, since $\langle H^i_{\rm STA} \rangle_\tau \geqslant 0$, $i = 1, 3$). Since power only characterizes the energy output of the engine, it is not directly impacted by the additional energy cost of the STA driving. It is only influenced by the shortcut through the reduction of the cycle time. For further reference, we additionally introduce the usual nonadiabatic efficiency of the engine, $\eta_{\rm NA} = -(\langle W_1 \rangle + \langle W_3 \rangle)/\langle Q_2 \rangle$, based on the formulas (1)–(3) in the absence of any STA protocol.

The power of the STA machine is, on the other hand,

$$P_{\rm STA} = -\frac{\langle W_1 \rangle_{\rm STA} + \langle W_3 \rangle_{\rm STA}}{\tau_{\rm cycle}}. \tag{8}$$

Since the STA protocol ensures adiabatic work output, $\langle W_i \rangle_{\rm STA} = \langle W_i \rangle_{\rm AD}$ $(i = 1, 3)$, in a shorter cycle duration $\tau_{\rm cycle}$, the superadiabatic power $P_{\rm STA}$ is always greater than the nonadiabatic power $P_{\rm NA} = -(\langle W_1 \rangle + \langle W_3 \rangle)/\tau_{\rm cycle}$ [40]. This ability to considerably enhance the power of a thermal machine is a key advantage of the STA approach. In the following, we explicitly evaluate the energetic cost of the STA driving, the efficiency (7), and the power (8) for the CD, LCD, and IE methods.

III. COUNTERDIABATIC DRIVING

We begin by analyzing the case of counterdiabatic driving, which was first introduced by Demirplak and Rice [21] and later independently developed by Berry [23]. The method has recently been implemented experimentally in a trapped-ion system [16]. The goal of counterdiabatic driving

(also called transitionless quantum driving) is to find a Hamiltonian $H_{\rm CD}$ for which the adiabatic approximation to the original Hamiltonian H_0 is the exact solution of the time-dependent Schrödinger equation for $H_{\rm CD}$. The explicit form of $H_{\rm CD}$ is

$$H_{\rm CD}(t) = H_0(t) + i\hbar \sum_n (|\partial_t n\rangle\langle n| - \langle n|\partial_t n\rangle |n\rangle\langle n|)$$
$$= H_0(t) + H_{\rm STA}^{\rm CD}(t), \tag{9}$$

where $|n\rangle = |n(t)\rangle$ denotes the nth eigenstate of the original Hamiltonian, $H_0(t)$, and $H_{\rm STA}^{\rm CD}$ is the STA driving Hamiltonian. For a time-dependent harmonic oscillator, it is given by [11,49]

$$H_{\rm SA}^{\rm CD}(t) = -\frac{\dot\omega_t}{4\,\omega_t}(xp + px). \tag{10}$$

The Hamiltonian (9) is quadratic in x and p, so it may be considered describing a generalized harmonic oscillator with a nonlocal operator [26,49,50]:

$$H_{\rm CD}(t) = \frac{p^2}{2m} + \left(-\frac{\dot\omega_t}{4\omega_t}\right)(xp + px) + \frac{m\omega_t^2 x^2}{2}. \tag{11}$$

Following Ref. [51], we may rewrite Eq. (11) as

$$H_{\rm CD}(t) = \hbar\Omega_t(b_t^\dagger b_t + 1/2) \tag{12}$$

with the instantaneous ladder operators b_t,

$$b_t = \sqrt{\frac{m\Omega_t}{2\hbar}}\left(\zeta_t x + \frac{ip}{m\Omega_t}\right), \tag{13}$$

and the effective frequency,

$$\Omega_t = \omega_t\sqrt{1 - \dot\omega_t^2/\left(4\omega_t^4\right)}, \tag{14}$$

with $\zeta_t = 1 + \dot\omega_t/(2i\omega_t\Omega_t)$. Note that $\Omega_t^2 > 0$ to avoid trap inversion in the process dynamics. This condition limits the rate of the frequency variation $\dot\omega_t$. Using the above equations, the adiabaticity parameter may be simply expressed as the ratio [51]

$$Q_{\rm CD}^*(t) = \frac{\omega_t}{\Omega_t}. \tag{15}$$

The adiabaticity parameter $Q_{\rm CD}^*$ is plotted as a function of the time t/τ for the compression step in Fig. 2 (the corresponding result for the expansion is simply the mirror image). We observe that $Q_{\rm CD}^*$ approaches the adiabatic value one at the end of the driving, as it should, and it is much smaller than the nonadiabatic $Q_{\rm NA}^*$, as expected.

We proceed by evaluating the mean energy of the effective harmonic oscillator (12) at any time t, assuming that it is initially in a thermal state $P_n^i = \exp(-\beta_i E_n^i)/Z_i$ at inverse temperature β_i. We obtain

$$\langle H_{\rm CD}(t)\rangle = \sum_n \hbar\omega_t(\langle m\rangle_{n,t} + 1/2)P_n^i$$
$$= \frac{\omega_t}{\omega_i}Q_{\rm CD}^*\langle H(0)\rangle, \tag{16}$$

where we have used the following expression for the mean quantum number, $\langle m\rangle_{n,t} + 1/2 = (n + 1/2)Q_{\rm CD}^*$ [46,47], and

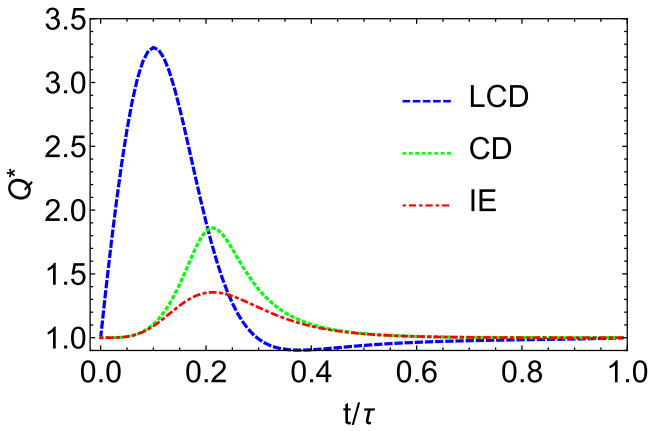

FIG. 2. Adiabaticity parameter Q^* for the compression step as a function of time for the three shortcut methods: counterdiabatic driving (CD), Eq. (15) (dotted green line); local counterdiabatic driving (LCD), Eq. (21) (dashed blue line); and inverse engineering (IE), Eq. (30) (dot-dashed red line) ($\omega_1/\omega_2 = 0.15$ and $\tau = 1.47$).

$\langle H(0)\rangle = \hbar\omega_i\coth(\beta\hbar\omega_i/2)/2$. The expectation value of the CD driving finally follows as

$$\left\langle H_{\rm STA}^{\rm CD}\right\rangle = \langle H_{\rm CD}(t)\rangle - \langle H_0(t)\rangle = \frac{\omega_t}{\omega_i}\langle H(0)\rangle\left(\frac{\omega_t}{\Omega_t} - 1\right), \tag{17}$$

where we used $\langle H_0(t)\rangle = \langle H(0)\rangle\omega_t/\omega_i$ [47]. We numerically compute the energetic cost of the STA driving as the time average of Eq. (17). This time average is different from zero, although $\langle H_{\rm STA}(t = (0, t_f))\rangle = 0$ in view of the boundary conditions (5). The corresponding efficiency [Eq. (7)] and power [Eq. (8)] are shown as a function of the driving time τ in Figs. 3 and 4 (dotted green lines).

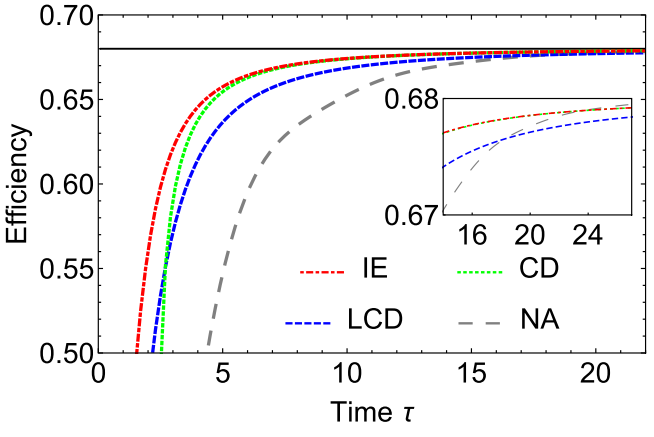

FIG. 3. Efficiency as a function of the driving time τ for the three shortcut methods: counterdiabatic driving (CD; dotted green line), local counterdiabatic driving (LCD; dashed blue line), and inverse engineering (IE; dot-dashed red line). The gray (large dashed) line shows the nonadiabatic efficiency (NA) without shortcut, while the black (solid) horizontal line is the adiabatic efficiency. Parameters are $\omega_1 = 0.32$, $\omega_2 = 1$, $\beta_1 = 0.5$, and $\beta_2 = 0.05$.

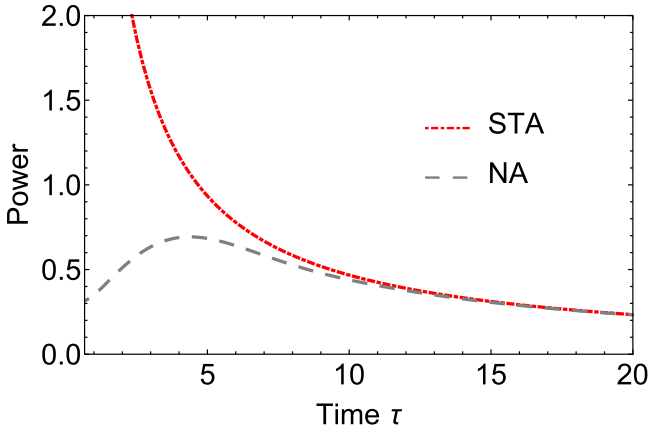

FIG. 4. Power as a function of the driving time τ for the three shortcut methods CD, LCD, and IE leads to the same power (dot-dashed red line). The gray (large dashed) line shows the nonadiabatic (NA) power. Same parameters as in Fig. 3.

IV. LOCAL COUNTERDIABATIC DRIVING

A limitation of the CD method is that it requires the knowledge of the spectral properties of the original Hamiltonian $H_0(t)$ at all times to construct the auxiliary term $H_{\rm STA}^{\rm CD}(t)$ in Eq. (9). A possibility to circumvent this problem is offered by the LCD approach [24,25], which has been experimentally demonstrated in Refs. [13,17,19]. Here the nonlocal operator (11) is mapped onto a unitarily equivalent Hamiltonian with a local potential by applying the canonical transformation $U_x = \exp(im\dot{\omega}_t x^2/4\hbar\omega)$, which cancels the cross terms xp and px. This leads to a new LCD Hamiltonian of the form [24,25]

$$H_{\rm LCD}(t) = U_x^\dagger(H_{\rm CD}(t) - i\hbar\dot{U}_x U_x^\dagger)U_x = \frac{p^2}{2m} + \frac{m\tilde{\Omega}_t^2 x^2}{2}, \tag{18}$$

with the modified time-dependent squared frequency

$$\tilde{\Omega}^2(t) = \omega_t^2 - \frac{3\dot{\omega}_t^2}{4\omega_t^2} + \frac{\ddot{\omega}_t}{2\omega_t}. \tag{19}$$

Hamiltonian (18) still drives the evolution along the adiabatic trajectory of the system of interest. By demanding that $H_{\rm LCD}(0,\tau) = H_0(0,\tau)$, and imposing $\dot{\omega}(\tau) = \ddot{\omega}(\tau) = 0$, the final state is equal for both dynamics, even in phase, and the final vibrational state populations coincide with those of a slow adiabatic process [24]. The frequency $\tilde{\Omega}^2(t)$ approaches $\omega^2(t)$ for very slow expansion and compression [25]. The LCD technique may be applied as long as $\tilde{\Omega}_t^2 > 0$, to avoid the trapping potential becoming a repeller. The expectation value of the local counterdiabatic Hamiltonian may be computed in analogy to the counterdiabatic driving and reads [40]

$$\langle H_{\rm LCD}(t)\rangle = \frac{\omega_t}{\omega_0}\left(1 - \frac{\dot{\omega}_t^2}{4\omega_t^4} + \frac{\ddot{\omega}_t}{4\omega_t^3}\right)\langle H(0)\rangle = \frac{\omega_t}{\omega_0} Q_{\rm LCD}^* \langle H(0)\rangle, \tag{20}$$

with the adiabaticity parameter

$$Q_{\rm LCD}^*(t) = 1 - \frac{\dot{\omega}_t^2}{4\omega_t^4} + \frac{\ddot{\omega}_t}{4\omega_t^3}. \tag{21}$$

The variation of the adiabaticity parameter as a function of t/τ is shown in Fig. 2. The expectation value of the LCD driving is moreover evaluated as before [40]:

$$\left\langle H_{\rm STA}^{\rm LCD}(t)\right\rangle = \langle H_{\rm LCD}(t)\rangle - \langle H_0(t)\rangle = \frac{\omega_t}{\omega_0}\langle H(0)\rangle\left[-\frac{\dot{\omega}_t^2}{4\omega_t^4} + \frac{\ddot{\omega}_t}{4\omega_t^3}\right]. \tag{22}$$

The corresponding numerically computed efficiency [Eq. (7)] and power [Eq. (8)] are shown as a function of the driving time τ in Figs. 3 and 4 (dashed blue lines).

V. INVERSE ENGINEERING

An additional STA method is based on the design of appropriate parameter trajectories of the frequency by employing the Lewis-Riesenfeld invariants of motion [52] supplemented by simple inverse-problem techniques [53]. The inverse engineering (IE) technique was first experimentally demonstrated in the decompression of an ultracold atomic gas in a harmonic trap under gravity [54] and later of a three-dimensional Bose-Einstein condensate at finite temperature [55]. For the time-dependent harmonic oscillator described by $H_0(t)$, the state dynamics will be the solution of the corresponding Schrödinger equation based on the invariants of motion of the following form [26,27]:

$$I(t) = \frac{1}{2}\left(\frac{x^2}{\bar{b}^2}m\omega_0^2 + \frac{1}{m}\pi^2\right), \tag{23}$$

where $\pi = \bar{b}p - m\dot{\bar{b}}x$ plays the role of a momentum conjugate to $x/\bar{b}$ and ω_0 is in principle an arbitrary constant. The dimensionless scaling function $\bar{b}_t = \bar{b}(t)$ satisfies the Ermakov equation,

$$\ddot{\bar{b}}_t + \omega_t^2\bar{b}_t = \omega_0^2/\bar{b}_t^3. \tag{24}$$

Its solutions should be chosen real to make I Hermitian. Whereas ω_0 is often rescaled to unity by a scale transformation of $\bar{b}_t$, another convenient choice is $\omega_0 = \omega(0)$. To achieve STA processes, $\omega(t)$ is first left undetermined and $\bar{b}_t$ is set to fulfill the equations $I(0) = H_0(0)$ and $[I(t_f), H_0(t_f)] = 0$. This guarantees that the eigenstates of I and H_0 are the same at the initial and final times and can be done by satisfying the boundary conditions

$$\begin{aligned} &\bar{b}(0) = 1, && \dot{\bar{b}}(0) = 0, && \ddot{\bar{b}}(0) = 0,\\ &\bar{b}(\tau) = \sqrt{\omega_0/\omega_f} = \gamma, && \dot{\bar{b}}(\tau) = 0, && \ddot{\bar{b}}(\tau) = 0, \end{aligned} \tag{25}$$

with $\omega_0 = \omega(0)$ and $\omega_f = \omega(\tau)$. For an individual eigenstate n of the oscillator Hamiltonian, the corresponding time-dependent instantaneous energy is

$$\langle H_{\rm IE}(t)\rangle_n = \frac{\hbar(n+1/2)}{2\omega_0}\left(\dot{\bar{b}}_t^2 + \omega_t^2\bar{b}_t^2 + \frac{\omega_0^2}{\bar{b}_t^2}\right). \tag{26}$$

The parameter ω_t is here deduced from the Ermakov equation (24). To ensure the noninversion of the trap and the ensuing divergence of the energetic cost, the condition $t_f > 1/(2\omega_f)$

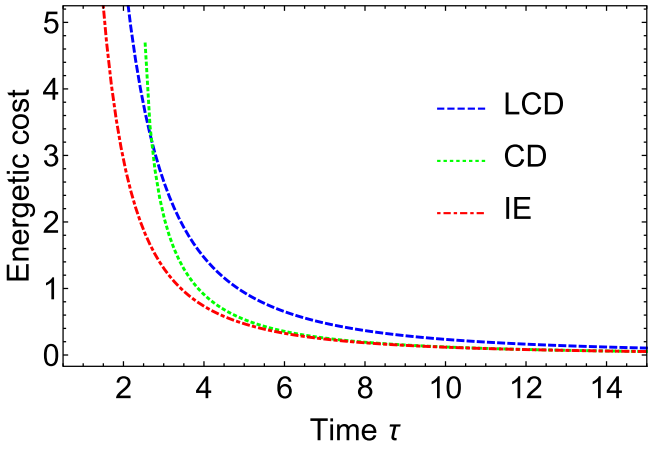

FIG. 5. Energetic cost of the STA protocol as a function the driving time τ for the three shortcut methods. Time-average of the expectation value of the STA Hamiltonian: counterdiabatic driving (CD), Eq. (17) (dotted green line); local counterdiabatic driving (LCD), Eq. (22) (dashed blue line); and inverse engineering (IE), Eq. (31) (dot-dashed red line). Same parameters as in Fig. 3.

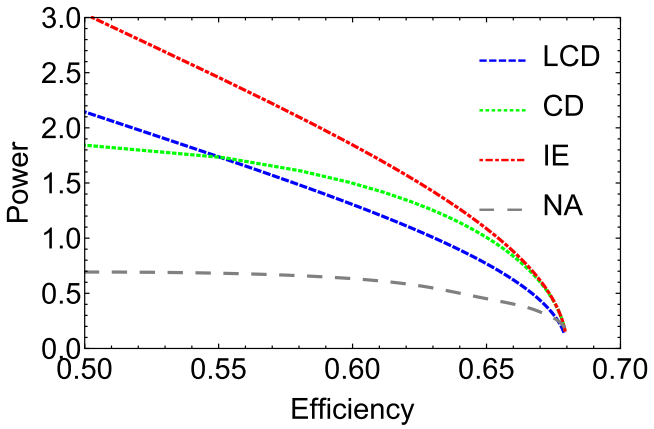

FIG. 6. Power-efficiency diagram for the three shortcut methods: counterdiabatic driving (CD; dotted green line), local counterdiabatic driving (LCD; dashed blue line), and inverse engineering (IE; dot-dashed red line). The gray (large dashed) line shows the nonadiabatic efficiency (NA) without shortcut. Same parameters as in Fig. 3.

should be satisfied. The expectation value of the STA at any given time follows as [26,27]

$$\langle H_{\rm IE}(t)\rangle = \frac{\hbar}{2}\left[\frac{\dot{\bar{b}}_t^2}{2\omega_0} + \frac{\omega_t^2\bar{b}_t^2}{2\omega_0} + \frac{\omega_0}{2\bar{b}_t}\right]\coth\left(\frac{\beta\hbar\omega_0}{2}\right). \quad (27)$$

Using the relation $\bar{b}_t = (\omega_0/\omega_t)^{1/2}$, we further have

$$\dot{\bar{b}}_t = -\frac{1}{2}\left(\frac{\omega_t}{\omega_0}\right)^{1/2}\frac{\omega_0\dot{\omega}_t}{\omega_t^2} \quad \text{and} \quad \dot{\bar{b}}_t^2 = \frac{1}{4}\frac{\omega_0\dot{\omega}_t^2}{\omega_t^3}. \quad (28)$$

Combining Eqs. (27) and (28), the time-dependent expectation value (27) can finally be written as

$$\begin{aligned}\langle H_{\rm IE}(t)\rangle &= \frac{\hbar}{2}\left[\frac{\dot{\omega}_t^2}{8\omega^3} + \frac{\omega_t}{2} + \frac{\omega_t}{2}\right]\coth\left(\frac{\beta\hbar\omega_0}{2}\right)\\ &= \frac{\omega_t}{\omega_0}\langle H(0)\rangle\left[1 + \frac{\dot{\omega}_t^2}{8\omega_t^4}\right]. \end{aligned} \quad (29)$$

The associated adiabaticity parameter hence reads

$$Q^*_{\rm IE}(t) = 1 + \frac{\dot{\omega}_t^2}{8\omega_t^4}, \quad (30)$$

as shown in Fig. 2 as a function of t/τ. We may again deduce the expectation value of the IE driving as

$$\left\langle H^{\rm IE}_{\rm STA}(t)\right\rangle = \langle H_{\rm IE}(t)\rangle - \langle H_0(t)\rangle = \frac{\omega_t}{\omega_0}\langle H(0)\rangle\frac{\dot{\omega}_t^2}{8\omega_t^4}. \quad (31)$$

The corresponding numerically computed efficiency [Eq. (7)] and power [Eq. (8)] are shown as a function of the driving time τ in Figs. 3 and 4 (dot-dashed red line).

VI. DISCUSSION AND CONCLUSIONS

We have performed a detailed analysis of the performance of a STA quantum harmonic heat engine, using three commonly employed techniques: CD, LCD, and IE. These three methods emulate adiabatic processes in finite time. We have first compared the time-dependent adiabaticity parameter $Q^*(t)$, Eqs. (15), (21)), and (30), for all three STA approaches (shown in Fig. 2). We observe that while all three methods lead to $Q^*(\tau) = 1$, per construction, the time dependence of $Q^*(t)$ may widely differ. The overall lowest value is achieved by IE, which therefore appears to be the most effective technique to reduce unwanted nonadiabatic transitions. The three STA strategies are clearly different. In the case of CD and LCD, STA is achieved by adding an additional term to the original Hamiltonian, while in the IE method, the time dependence of the parameters of the original Hamiltonian is engineered. The latter technique seems to offer more flexibility (different invariants and different phase functions to be chosen) and in turn a better STA protocol. The IE approach leads to an overall smaller adiabaticity parameter (as seen in Fig. 2), with an overall lower energetic cost of driving (see Fig. 5).

We have further numerically calculated the energetic cost of the STA driving as the time average of the expectation value of the respective STA Hamiltonians, given in Eqs. (17), (22), and (31). The corresponding efficiencies and powers that take into account this energetic cost are presented in Figs. 3 and 4. We first note that all three methods lead to a significant increase of the efficiency at short cycle times, compared to the standard NA engine without shortcut. We observe furthermore that they all simultaneously yield a large enhancement of the power in the same regime. STA engines thus always outperform their traditional counterparts for short cycle durations. This is a remarkable feature of STA boosted quantum heat engines. They hence appear as energy efficient thermal machines that are able to produce more output from the same input at higher power. This property follows from the fact that STA protocols, on the one hand, speed up the dynamics (therefore increasing power), and on the other hand, also ensure that the final state is an adiabatic state instead of a highly excited state (thus reducing entropy production and consequently increasing efficiency).

Our study finally establishes that among the three considered STA methods, IE offers the largest increase of

efficiency. This result confirms and directly follows from our previous observation that IE is the most effective method to suppress nonadiabatic transitions. At the same time, all three approaches yield the same enhanced power, since they produce the adiabatic work output in much less time. These findings are illustrated in the power-efficiency diagram shown in Fig. 6. The latter clearly demonstrates the advantage of STA heat engines operating in finite time.

ACKNOWLEDGMENTS

This work was partially supported by the EU Collaborative Project TherMiQ (Grant Agreement 618074). O.A. was supported by the Royal Society Newton International Fellowship (Reference No. NF160966) and the Royal Commission for the 1851 Exhibition.

[1] H. B. Callen, *Thermodynamics and an Introduction to Thermostatistics* (Wiley, New York, 1985).
[2] Y. A. Cengel and M. A. Boles, *Thermodynamics: An Engineering Approach* (McGraw-Hill, New York, 2001).
[3] B. Andresen, P. Salamon, and R. S. Berry, Phys. Today **37**, 62 (1984).
[4] B. Andresen, Angew. Chem. Int. Ed. **50**, 2690 (2011).
[5] N. Shiraishi, K. Saito, and H. Tasaki, Phys. Rev. Lett. **117**, 190601 (2016).
[6] T. Feldmann and R. Kosloff, Phys. Rev. E **61**, 4774 (2000).
[7] Y. Rezek and R. Kosloff, New. J. Phys. **8**, 83 (2006).
[8] J. Rossnagel, O. Abah, F. Schmidt-Kaler, K. Singer, and E. Lutz, Phys. Rev. Lett. **112**, 030602 (2014).
[9] O. Abah and E. Lutz, Europhys. Lett. **113**, 60002 (2016).
[10] American Physical Society Energy Efficiency Report, 2008 (unpublished), http://www.aps.org/energyefficiencyreport.
[11] E. Torrontegui, S. Ibáñez, S. Martínez-Garaot, M. Modugno, A. del Campo, D. Guéry-Odelin, A. Ruschhaupt, X. Chen, and J. G. Muga, Adv. At. Mol. Opt. Phys. **62**, 117 (2013).
[12] S. Deffner, C. Jarzynski, and A. del Campo, Phys. Rev. X **4**, 021013 (2014).
[13] M. G. Bason, M. Viteau, N. Malossi, P. Huillery, E. Arimondo, D. Ciampini, R. Fazio, V. Giovannetti, R. Mannella, and O. Morsch, Nat. Phys. **8**, 147 (2012).
[14] R. Bowler, J. Gaebler, Y. Lin, T. R. Tan, D. Hanneke, J. D. Jost, J. P. Home, D. Leibfried, and D. J. Wineland, Phys. Rev. Lett. **109**, 080502 (2012).
[15] A. Walther, F. Ziesel, T. Ruster, S. T. Dawkins, K. Ott, M. Hettrich, K. Singer, F. Schmidt-Kaler, and U. Poschinger, Phys. Rev. Lett. **109**, 080501 (2012).
[16] S. An, D. Lv, A. del Campo, and K. Kim, Nat. Commun. **7**, 12999 (2016).
[17] J. Zhang, J. H. Shim, I. Niemeyer, T. Taniguchi, T. Teraji, H. Abe, S. Onoda, T. Yamamoto, T. Ohshima, J. Isoya, and D. Suter, Phys. Rev. Lett. **110**, 240501 (2013).
[18] Y.-X. Du, Z.-T. Liang, Y.-C. Li, X.-X. Yue, Q.-X. Lv, W. Huang, X. Chen, H. Yan and S.-L. Zhu, Nat. Commun. **7**, 12479 (2016).
[19] S. Deng, A. Chenu, P. Diao, F. Li, S. Yu, I. Coulamy, A. del Campo, and H. Wu, Sci. Adv. **4**, eaar5909 (2018).
[20] I. Martinez, A. Petrosyan, D. Guery-Odelin, E. Trizac, and S. Ciliberto, Nat. Phys. **12**, 843 (2016).
[21] M. Demirplak and S. A. Rice, J. Phys. Chem. A **107**, 9937 (2003).
[22] M. Demirplak and S. A. Rice, J. Chem. Phys. B **109**, 6838 (2005).
[23] M. V. Berry, J. Phys. A: Math. Theor. **42**, 365303 (2009).
[24] S. Ibáñez, X. Chen, E. Torrontegui, J. G. Muga, and A. Ruschhaupt, Phys. Rev. Lett. **109**, 100403 (2012).
[25] A. del Campo, Phys. Rev. Lett. **111**, 100502 (2013).
[26] X. Chen, A. Ruschhaupt, S. Schmidt, A. del Campo, D. Guéry-Odelin, and J. G. Muga, Phys. Rev. Lett. **104**, 063002 (2010).
[27] X. Chen and J. G. Muga, Phys. Rev. A **82**, 053403 (2010).
[28] J. Deng, Q.-h. Wang, Z. Liu, P. Hänggi, and J. Gong, Phys. Rev. E **88**, 062122 (2013).
[29] Z. C. Tu, Phys. Rev. E **89**, 052148 (2014).
[30] A. del Campo, J. Goold, and M. Paternostro, Sci. Rep. **4**, 6208 (2014).
[31] M. Beau, J. Jaramillo, and A. del Campo, Entropy **18**, 168 (2016).
[32] J. Jaramillo, M. Beau, and A. del Campo, New. J. Phys. **18**, 075019 (2016).
[33] L. Chotorlishvili, M. Azimi, S. Stagraczynski, Z. Toklikishvili, M. Schüler, and J. Berakdar, Phys. Rev. E **94**, 032116 (2016).
[34] A. C. Santos, R. D. Silva, and M. S. Sarandy, Phys. Rev. A **93**, 012311 (2016).
[35] Y. Zheng, S. Campbell, G. De Chiara, and D. Poletti, Phys. Rev. A **94**, 042132 (2016).
[36] I. B. Coulamy, A. C. Santos, I. Hen, and M. S. Sarandy, Front. ICT **3**, 19 (2016).
[37] S. Campbell and S. Deffner, Phys. Rev. Lett. **118**, 100601 (2017).
[38] K. Funo, J.-N. Zhang, C. Chatou, K. Kim, M. Ueda and A. del Campo, Phys. Rev. Lett. **118**, 100602 (2017).
[39] E. Torrontegui, I. Lizuain, S. González-Resines, A. Tobalina, A. Ruschhaupt, R. Kosloff, and J. Muga, Phys. Rev. A **96**, 022133 (2017).
[40] O. Abah and E. Lutz, Europhys. Lett. **118**, 40005 (2017).
[41] R. Kosloff, J. Chem. Phys. **80**, 1625 (1984).
[42] E. Geva and R. Kosloff, J. Chem. Phys. **96**, 3054 (1992).
[43] B. Lin and J. Chen, Phys. Rev. E **67**, 046105 (2003).
[44] H. T. Quan, Y. X. Liu, C. P. Sun, and F. Nori, Phys. Rev. E **76**, 031105 (2007).
[45] R. Kosloff and Y. Rezek, Entropy **19**, 136 (2017).
[46] S. Deffner and E. Lutz, Phys. Rev. E **77**, 021128 (2008).
[47] S. Deffner, O. Abah, and E. Lutz, Chem. Phys. **375**, 200 (2010).
[48] K. Husimi, Prog. Theor. Phys. **9**, 381 (1953).
[49] J. G. Muga, X. Chen, S. Ibáñez, I. Lizuain, and A. Ruschhaupt, J. Phys. B **43**, 085509 (2010).
[50] M. V. Berry, J. Phys. A: Math. Gen. **18**, 15 (1985).
[51] H. Mishima and Y. Izumida, Phys. Rev. E **96**, 012133 (2017).
[52] H. R. Lewis and W. B. Riesenfeld, J. Math. Phys. **10**, 1458 (1969).
[53] J. P. Palao, J. G. Muga, and R. Sala, Phys. Rev. Lett. **80**, 5469 (1998).
[54] J. F. Schaff, X. L. Song, P. Vignolo, and G. Labeyrie, Phys. Rev. A **82**, 033430 (2010).
[55] J. F. Schaff, X. L. Song, P. Capuzzi, P. Vignolo, and G. Labeyrie, Europhys. Lett. **93**, 23001 (2011).